the overall thermohaline circulation itself. Indeed, the role of interior mixing in the thermohaline circulation can be compared to the role of the wind stress in the wind-driven circulation; that is, turbulence provides the essential interior balance of vertical upwelling with downward mixing of heat, just as the wind stress pattern at the surface imparts circulation to the ocean's horizontal gyres. The high latitude sinking regions are then analogs of the western boundary currents that close the wind-driven flows. This view more clearly shows that it is the interior mixing acting on available density gradients, rather than the surface formation of dense water, that acts as the driving agent for the thermohaline circulation. Indeed, without mixing, the deep circulation would become cold and stagnant and oceanic warmth would be confined to a thin surface boundary layer. This issue is of major concern, since the substantial circulation of warm water poleward is responsible for much of the heat flux carried by the ocean. There is evidence that the North Atlantic limb of the thermohaline circulation was cut off at various times in the past, and some suggest that global warming could shut it off in future, due to surface water freshening by an enhanced hydrologic cycle. Recent modeling work shows that there is a delicate balance between the fresh water forcing and the rate of interior mixing that determines the stability of the thermohaline circulation. A better understanding of oceanic mixing is thus essential for prediction of the future evolution of the Earth's climate system.

See also

Double-diffusive Convection. Internal Tidal Mixing. Thermohaline Circulation. Tracer Release Experiments. Upper Ocean Mixing Processes.

Further Reading

Ledwell JL *et al.* (2000). Evidence for enhanced mixing over rough topography in the abyssal ocean. *Nature* 403: 179–182.

Munk W and Wunsch C (1998). Abyssal recipes II: Energetics of tidal and wind mixing. *Deep-Sea Research* 45: 1977–2010.

Polzin KL, Toole JM, Ledwell JR and Schmitt RW (1997). Spatial variability of turbulent mixing in the abyssal ocean. *Science* 276: 93–96.

DISPERSION FROM HYDROTHERMAL VENTS

K. R. Helfrich, Woods Hole Oceanographic Institution, Woods Hole, MA, USA

doi:10.1006/rwos.2001.0115

Introduction

Among the most significant scientific events of the last century is the discovery of hydrothermal vent fields and their unusual ecological communities along the crests of the mid-ocean ridges. The venting consists of localized sources of very hot ($\sim$350°C) water that rises 100–300 m above the vent before it spreads laterally, similar to the plume from a smokestack. Venting also occurs as less intense and relatively cool diffuse flow ($\sim$10°C above the ambient ocean temperature) spread out over a much broader area than the focused high-temperature vents. Diffuse flow rises only a few meters above the seafloor before it is mixed with the ambient sea water. While the diffuse flow carries about half of the total hydrothermal heat flux, its effect on the overlying water column is much less dramatic than the high-temperature vents.

The hydrothermal venting from diffuse and localized high-temperature venting is essentially continuous over periods of years to decades. On longer timescales the individual vent sites will dissipate and new sites will emerge at other locations along the ridge crest. This nearly continuous venting is also punctuated by intense short duration venting events. These intense events are produced by magma eruptions on the seafloor or tectonic activity that rapidly exposes large quantities of sea water to hot rock or releases large quantities of very hot water from the crust. The result is the creation of huge 'mega plumes' that can rise 500–1000 m above the ridge crest to form mesoscale eddies with diameters of O(20 km) and thickness of O(500 m).

Because of its large buoyancy and the dynamical control exerted by the Earth's rotation, vent fluid is not simply advected away by background flow. The venting is capable of forcing circulation on a variety of temporal and spatial scales and this may have important consequences on how the vent fluid is ultimately dispersed. This article focuses on the flow

produced by high-temperature venting and megaplumes, since they are most relevant for long-range dispersal of vent fluids as a consequence of their large vertical penetration into the water column.

The fate of the heat, chemicals, and biological material released by the vent is of interest for many reasons. To geophysicists, the hydrothermal heat flux represents a substantial fraction of the total heat flux (conductive plus convective) from mid-ocean ridges. For chemists, the vent fluid is laden with chemicals and minerals leeched from the subseafloor rock that over geologic time may contribute to the geochemical state of the oceans. The unique biological communities that accompany venting depend upon the chemical and thermal energy delivered by the venting. Since most of these unusual animals can survive only at vent sites, the dispersal of vent fluid is the primary mechanism of larvae dispersal and the colonization of remote new vent sites.

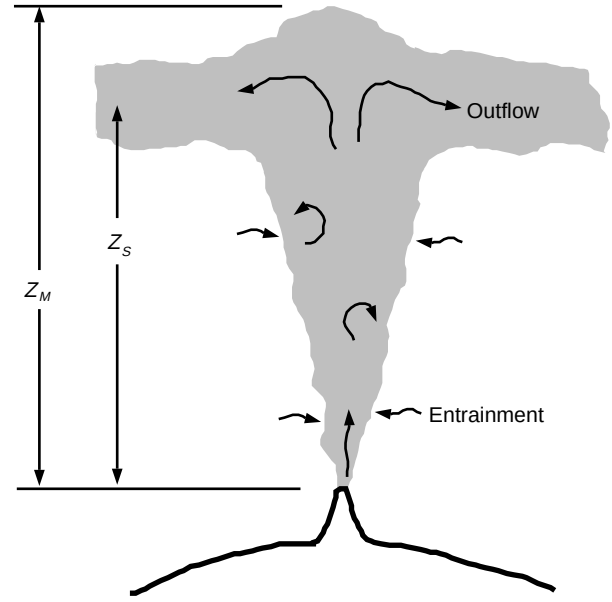

Figure 1 Sketch of a plume from a localized high-temperature hydrothermal vent. The plume rises to a maximum height Z_M above the source. The rising stem of the plume continually entrains ambient fluid so that the density of the plume buoyancy decreases with height above the bottom. Eventually the plume density equals the ambient density and it spreads laterally at some height Z_S above the source.

The Rising Plume

The cascade of scales initiated by a high-temperature vent begins with the fast $O(1\,\text{h})$ rise of the buoyant fluid from the vent to the spreading level $O(100\,\text{m})$ above the source. Fluid emerging from an isolated hot vent rises as a turbulent plume, entraining and mixing with the ambient sea water as it rises (see **Figure 1**). Because the entrained ambient water is denser than the fluid in the turbulent plume, the plume buoyancy decreases continually with height above the source. If the ambient environment had uniform density the plume fluid would remain less dense than the environment and it would rise indefinitely. However, even in the deep ocean the ambient water is stratified. Eventually the plume density increases until it equals the background density. After a short overshoot of this neutral density level due to the momentum of the rising fluid, the plume spreads horizontally as an intrusive density current, or it may be swept downstream by ambient currents.

Figure 2 shows a transect through a hydrothermal plume on the Juan de Fuca Ridge in the North Pacific. The figure is typical of many such observations made worldwide over the last two decades. In the figure temperature and light attenuation anomalies (defined relative to the background values along isolines of density) are contoured as functions of depth and horizontal distance along the centerline of the axial valley. High values of light attenuation anomaly are due to particulates introduced into the water column by venting. Indeed, in many cases light attenuation is a more useful indicator of hydrothermal activity than temperature anomaly. As discussed below, the temperature anomaly may be very small, or even negative.

The main features of the buoyant rise, entrainment, and spreading processes can be determined with a theoretical plume model that conserves momentum, mass, and buoyancy integrated on a horizontal slice across the plume. The key assumption is that the entrainment velocity, or the rate at which ambient fluid is drawn into the plume, is linearly proportional to the vertical velocity within the plume. (Details of the basic plume models and the justification of the assumptions are discussed in Morton *et al.* (1956), see Further Reading section.)

Modeling, laboratory experiments, and observations show that the maximum rise height the plume above the source Z_M is given by:

$$Z_M = 3.8(F_0 N^{-3})^{1/4} \qquad [1]$$

where

$$F_0 = Qg\left(\frac{\rho_0 - \rho_s}{\rho_0}\right) \qquad [2]$$

and

$$N^2 = \frac{-g}{\rho_0}\frac{d\rho_a}{dz} \qquad [3]$$

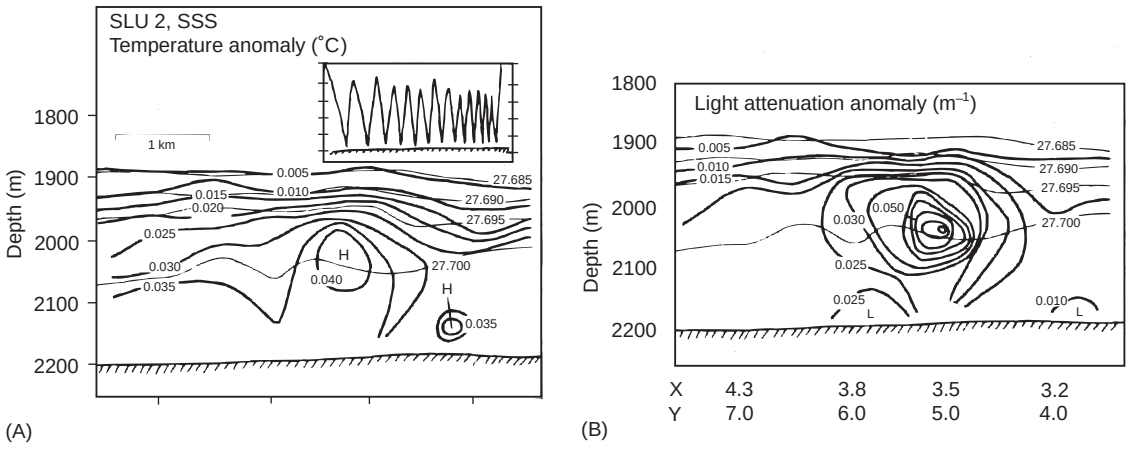

Figure 2 Transect of temperature (A) and light attenuation (B) anomalies through a hydrothermal plume on the Juan de Fuca Ridge in the North Pacific. The transect was taken along the axis of the axial valley. The maxima of temperature and light attenuation are located directly over the vent. (Reproduced with permission from Baker and Massoth, 1987).

Here F_0 is the buoyancy flux from the vent and N is the buoyancy frequency of the ambient water, which over the rise height of the plume is assumed to be constant. Q is the source volume flux and ρ_s (ρ_0) is the source (ambient) fluid at the level of the vent. The background density is $\rho_a(z)$, z is the height above the source, and g is the acceleration due to gravity.

While the maximum plume rise is Z_M, the radial outflow is centered at a slightly lower height $Z_S \approx 0.8Z_M$. The thickness of the spreading layer over the source is $\approx 0.2Z_M$. Typical values of $F_0 = 10^{-2}\,\mathrm{m^4\,s^{-3}}$ and $N = 10^{-3}\,\mathrm{s^{-1}}$ give $Z_M \approx 210\,\mathrm{m}$. The time taken for a parcel of fluid to ascend from the vent to the spreading level $\sim N^{-1}$. Doubling the vent buoyancy flux leads to only a very minor change in Z_M. This weak quarter power dependency on F_0 is significant because observation of Z_M and N are often used to estimate the heat flux from a vent $H = \rho_s c_p Q(T_s - T_0) = \rho_s c_p F_0/g\alpha$, where c_p is the specific heat, α is the coefficient of thermal expansion and T_s and T_0 are the temperatures of the source and ambient fluids, respectively. From eqn [1], $H \propto Z_M^4 N^3$. Estimates of H are very sensitive to small errors in either Z_M or N.

The model and eqn [1] were derived under ideal conditions. Others effects will affect plume behavior. For example, in an ambient flow with velocity U, $Z_M \propto (F_0 U^{-1} N^{-2})^{1/3}$. Increasing U leads to decreasing rise heights. Mid-ocean ridge crests are locations of rough, variable topography and this may affect plume behavior. For example, the slow spreading Mid-Atlantic Ridge is characterized by axial valleys that are typically deeper than the plume rise spreading level, Z_S, while the fast spreading Pacific ridges have axial valleys shallower than Z_S. Deep-valley topography will constrain the plume outflow and direct it along the ridge axis, limiting off-ridge dispersal of vent fluids.

Despite limitations the basic plume model provides useful insight into the dispersal of vent fluids. The entrainment of ambient water into the plume causes a substantial dilution of a parcel of vent fluid. The volume flux into the spreading level $Q_M = 1.3(F_0^3 N^{-5})^{1/4}$. For $F_0 = 10^{-2}\,\mathrm{m^4\,s^{-3}}$ and $N = 10^{-3}\,\mathrm{s^{-1}}$, $Q_M = O(10^2\,\mathrm{m^3\,s^{-1}})$. This gives a dilution of $O(10^4)$ for a typical source flux $Q = O(10^{-2}\,\mathrm{m^3\,s^{-1}})$. Entertainment occurs at all levels, but the largest velocities of background fluid into the plume occur in the lower quarter of the rise height. Larvae of bottom dwelling vent organisms can easily be swept into the plume and rapidly transported up to the spreading level. They then have a greater likelihood of dispersal over the distances typical of individual vent spacing ($O(10\,\mathrm{km})$), Furthermore, these larvae are in water that is chemically distinct from the ambient environment and this may enhance survival during the dispersal process.

The temperature and salinity anomalies at the spreading level (where the density anomaly is zero) are dependent on the ambient temperature and salinity gradients and can be counter-intuitive. In the deep Pacific salinity decreases with height above the bottom, as does temperature. These background gradients results in relatively warm and salty spreading plume water. An example of the temperature and salinity vertical profiles through the effluent layer of a plume on the Juan de Fuca Ridge is shown in **Figure 3**. The spreading plume is easily

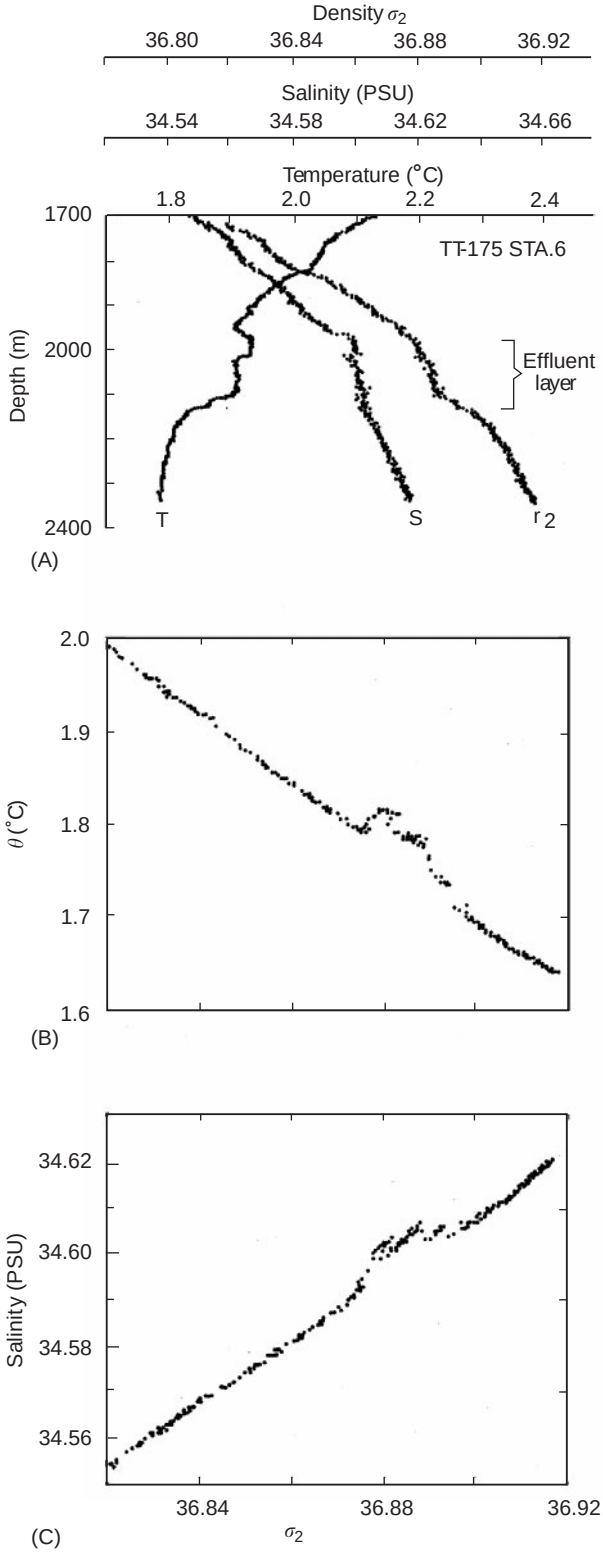

Figure 3 (A) Vertical profiles of temperature, salinity and density through a hydrothermal effluent layer on the Juan de Fuca Ridge. The relatively warm and salty effluent layer is clear in plots of potential temperature, θ, versus potential density, σ_2 (B) and salinity versus density (C). (Reproduced with permission from Lupton *et al.*, 1985.)

distinguished as a layer of nearly uniform temperature and salinity in **Figure 3**A. In **Figure 3**B and C the potential temperature θ and salinity are plotted against potential density, σ_2, and clearly show the relatively warm and salty effluent layer. In comparison, in the deep Atlantic where the salinity increases with height above the bottom the spreading plume is relatively cold and fresh. The temperature of the plume at the neutral level is colder than the ambient water despite the enormous temperature of the source fluid. Thus temperature alone may not always be an obvious indicator of hydrothermal activity. In either case, temperature anomalies at the spreading level are $O(10^{-1}\,^{\circ}\mathrm{C})$ despite source temperature anomalies of $\sim 350^{\circ}\mathrm{C}$.

The rise characteristics of event megaplumes are similar to the continuous venting, except that the source duration is limited and the buoyancy flux, F_0, is typically one to two orders of magnitude larger. For comparison, the heat flux from a typical high temperature vent is 1–100 MW, while megaplume sources are estimated to be > 1000 MW. If the source duration is small compared with the parcel rise time, N^{-1}, then the plume model must be replaced by a model for an isolated thermal. In this case $Z_M = 2.7(B_0 N^{-2})^{1/4}$, where $B_0 = V_0 g(\rho_0 - \rho_s/\rho_0)$ is the buoyancy and V_0 the volume of the pulse of hot fluid forming the release. Entrainment into and dilution of a thermal are comparable to the continuous release.

Mesoscale Flow and Vortices

A high temperature vent continuously delivers plume fluid to the spreading level. Ambient currents can simply advect this fluid away from the vent location, but if the currents are weak, or oscillatory with small mean, then plume fluid accumulates over the vent and a radial outflow must develop. On a timescale f^{-1} this radial flow will be retarded by rotation. Here $f = 2\,\Omega \sin(\phi)$ is the Coriolis parameter, Ω is the rotation rate of Earth and ϕ the latitude. At $45^{\circ}\mathrm{N}$ $f = 10^{-4}\,\mathrm{s}^{-1}$. The outward-flowing fluid parcels turn to the right (looking from above in the northern hemisphere) and an anticyclonic circulation will develop. With time a slowly growing lens of plume fluid will be formed. Below the spreading level, entrainment into the rising limb of the plume causes a radial inflow of ambient water. The Coriolis acceleration again results in fluid parcels turning to the right as they move inward and cyclonic circulation is established. The result is a baroclinic vortex pair: an anticyclonic lens of plume fluid at the spreading level and cyclonic circulation of ambient fluid around the rising

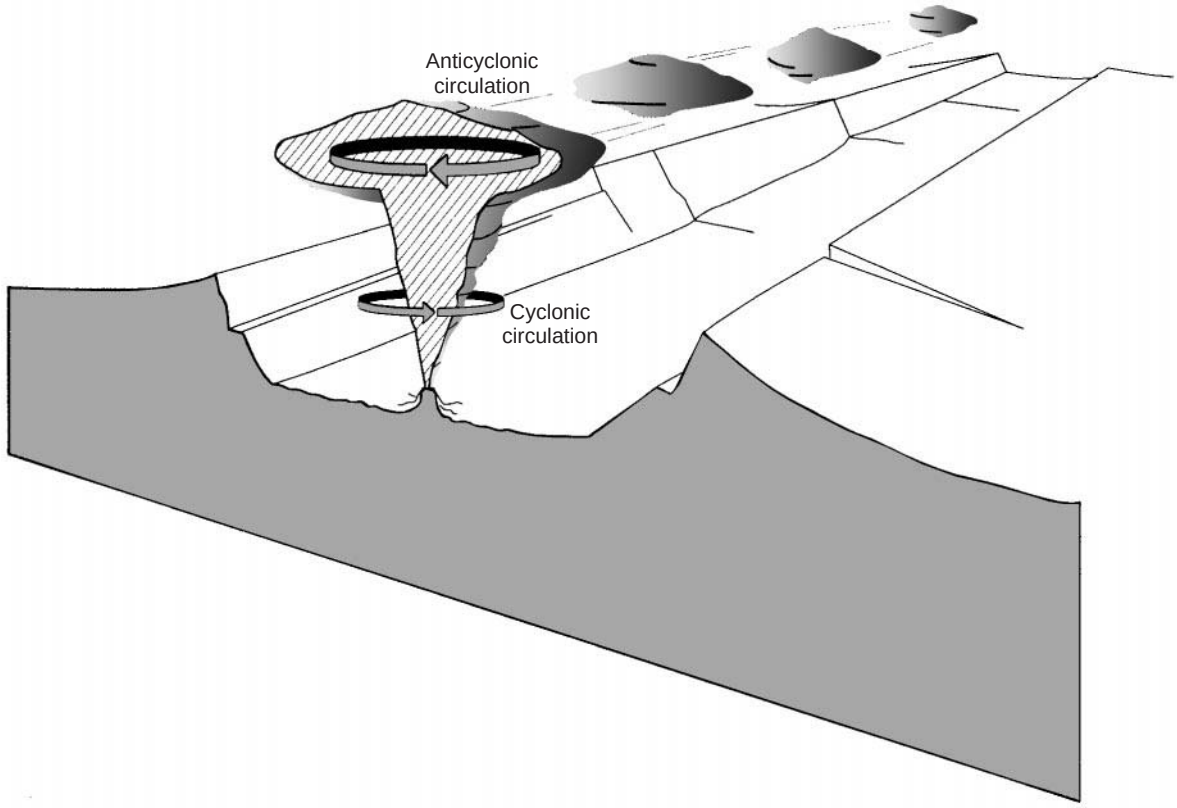

Figure 4 Sketch of the effect of the Earth's rotation on a hydrothermal plume. Rotation causes an anticyclonic horizontal circulation in the spreading fluid and cyclonic circulation below. These flows are indicated by the arrows. Lateral spreading of plume fluid is retarded by rotation and eventually the plume may become unstable, producing isolated vortices of plume fluid which have a radius $L \approx Z_M N/f$, which is about 2 km at mid-latitudes. A continuous vent could result in the production of numerous eddies which propagate away from the vent site.

buoyant plume. This circulation is sketched in **Figure 4**. The dynamical balance is geostrophic wherein the radial pressure gradients are balanced by the Coriolis acceleration.

Figure 5 shows results from a laboratory experiment that illustrates the effects of rotation on plume structure. In the photographs dense fluid, dyed for visualization, is released from a small source into a tank of water that has been stratified with salt to give a constant density gradient (constant N). The tank is on a table rotating about the vertical axis to simulate the Coriolis effect. These photographs are taken looking in from the side a short time after the source has been turned on. The experiments were done with dense fluid which falls, rather than light fluid that rises. This is inconsequential for the physics and the hydrothermal vent situation can be envisioned simply by turning the figures upside down. As the rotation increases, as measured by decreasing values of the ratio N/f, lateral spreading of the plume is retarded and the anticyclonic lens of plume fluid becomes thicker. Dynamical scaling arguments and experiments show that the aspect ratio of the resulting eddy, $h/L \approx 0.75\, f/N$. Here h is the central thickness of the anticyclonic eddy (dyed fluid in the figure) and L is the radius. These arguments also give the eddy azimuthal, or swirling, velocity $v \sim (F_0 f)^{1/4}$. For the typical values of F_0 and $f = 10^{-4}\,\mathrm{s}^{-1}$, $v \sim 0.03\,\mathrm{m\,s}^{-1}$. This is comparable to observed background flows over ridges and suggests that plume vortex flow can persist in the presence of a background flow.

The anticyclonic plume eddy will continue to grow until it reaches a critical radius $L \approx Z_M N/f$ at which it becomes unstable and breaks up. An example of plume break up is shown in **Figure 6**, which contains a sequence of photographs looking down on the experiment. The plume vortex was initially circular (not shown), but eventually the eddy elongates (**Figure 6**A). It then splits into two separate vortex pairs (**Figure 6**B) which propagate away from the source (**Figure 6**C). The process of formation and instability process then begin again. A steady source results in the unsteady production

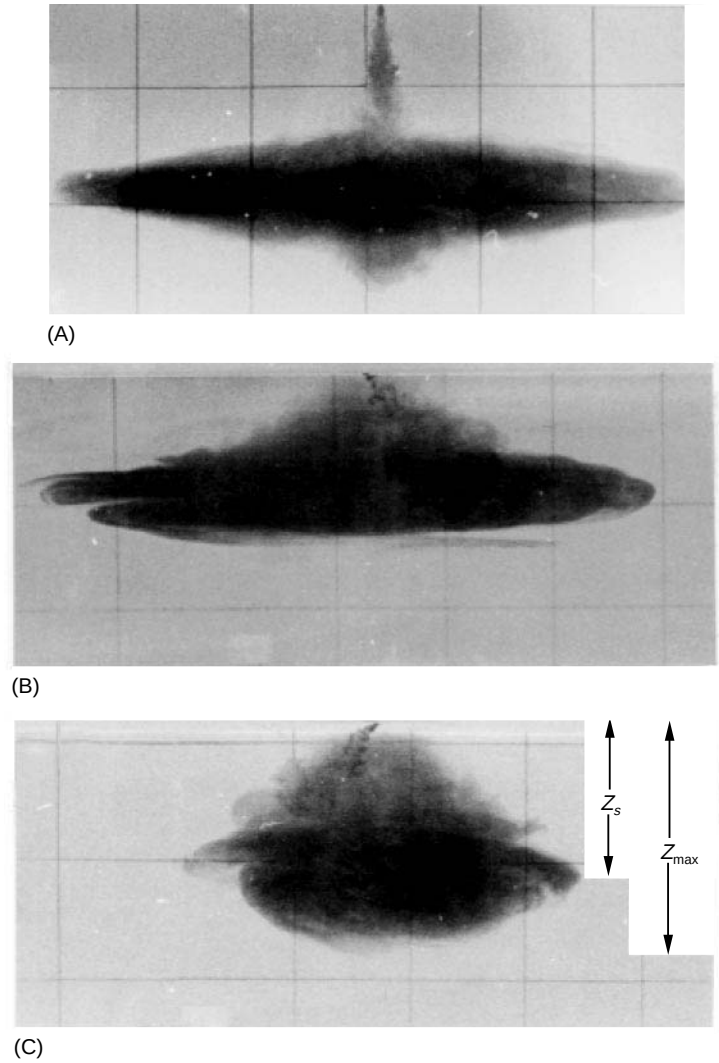

Figure 5 Side-view photographs showing the effects of rotation on convective plumes. In (A) the rotation is zero. The classic turbulent plume and spreading layer are evident. Panel (B) has weak rotation, $N/f = 5.02$. The lateral spreading is inhibited and the falling plume is partially obscured by the cyclonic circulation which has developed around the plume. In (C) the rotation is stronger, $N/f = 1.42$, and the anticyclonic lens of dyed fluid is thicker and has a smaller radius. See the text for a description of the experiment. (Reproduced with permission from Helfrich and Battisti, 1991.)

of vent vortices as depicted in **Figure 4**. The time-scale for this production process is $t_B \sim 10^2 N f^{-2}$. For typical mid-latitude values of N and f and Z_M, $L \approx 2\,\text{km}$ and $t_B \sim 2$ months. Note that f decreases as the equator is approached, resulting in larger diameter eddies which take longer to grow if other factors remain constant.

The small size and long production time contribute to difficulty in directly observing these eddies, although observations of the water column properties do show indications of eddy-like features with the expected scales. Futhermore, ambient flows can be expected to influence this idealized scenario. But even with ambient flows that would tend to carry plume fluid from a vent, the tell-tale anticyclonic circulation at the spreading level and cyclonic flow below is expected. Indeed, there is observational evidence for this vorticity signature in time mean measurements of flow in the vicinity of a vent. However, the most compelling evidence for this dynamical scenario comes from megaplume observations. **Figure 7** shows temperature and light attenuation (a measure of particulate concentration indicative of hydrothermal source fluid) anomaly sections across a megaplume observed near the Juan de Fuca Ridge in the North Pacific. Note the much larger rise height and lateral scales of this plume compared with the example in **Figure 2**. The

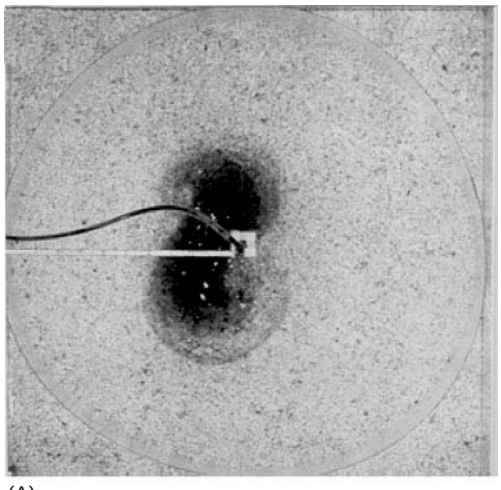

(A)

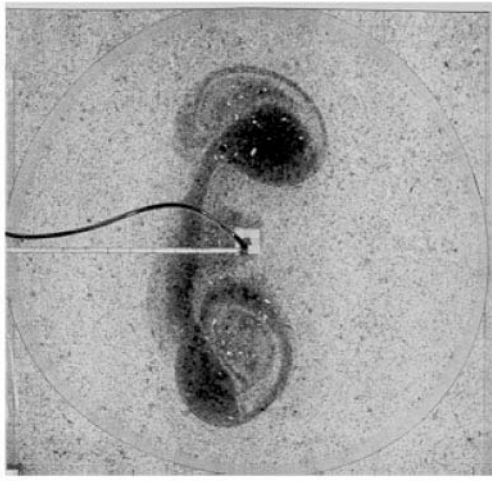

(B)

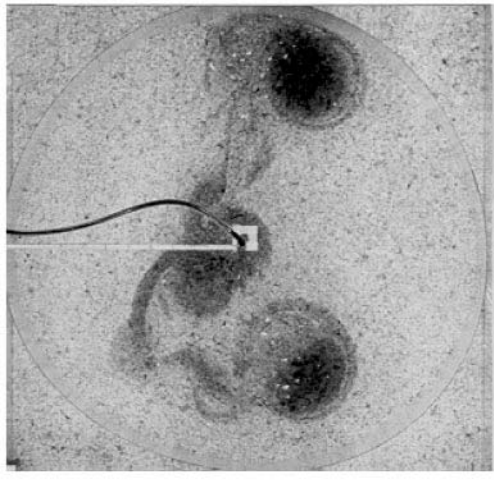

(C)

Figure 6 Photographs of a laboratory experiment showing the formation and break up of a plume vortex. The view is from above and time increases from panel (A) to (C). A single continuous source produces one plume vortex which eventually becomes unstable (A), and forms two smaller baroclinic vortex pairs which move away from the source (B), after which the process of plume vortex formation begins again (C). (Reproduced with permission from Helfrich and Battisti, 1991.)

structure of the megaplume is indicative of anticyclonic circulation within the core and this has been confirmed by detailed analysis.

The production of eddies from either continuous high temperature venting or episodic megaplume events is important for the dispersal of the vent fluid. While dispersal by simple advection and stirring by prevailing flows may be the dominant dispersal mechanism, even occasional eddy formation is significant. Coherent anticyclonic vortices are known to have closed streamlines and can retain their anomalous properties over long distances and large time periods. These eddies provide a mechanism for the long-range dispersal of vent organisms

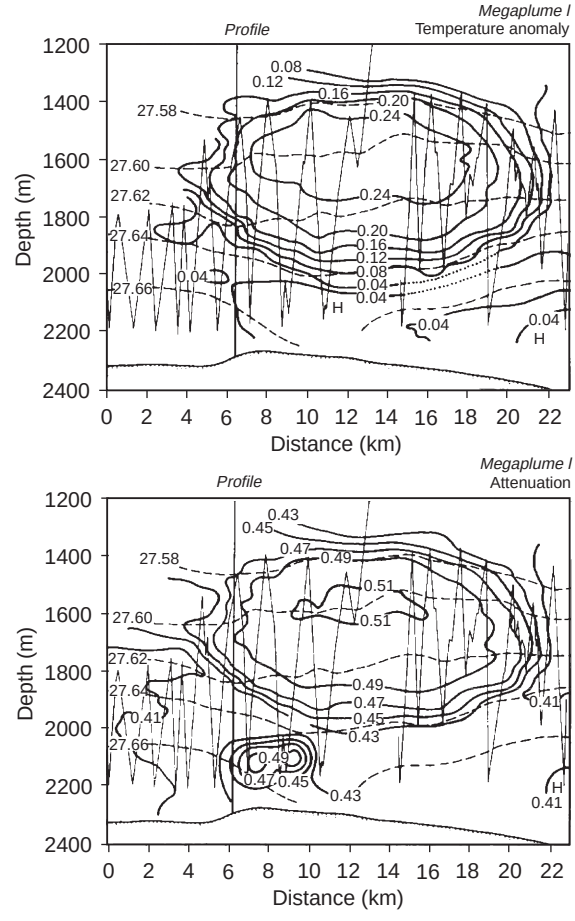

Figure 7 Observations of the temperature and light attenuation anomalies of a megaplume found near the Juan de Fuca Ridge. The figure shows a slice in depth and horizontal distance through the center of a nearly circular (in plan view) plume. The eddy aspect ratio $b/L \sim f/N$ as predicted by the scaling theory and laboratory experiments. The lower level high in light attenuation may be the result of a separate, less intense hydrothermal source. The horizontal dashed lines are density isolines (σ_θ contours) and the saw-tooth lines indicate the trajectory of the measurement package. (Reproduced with permission from Baker *et al.*, 1989.)

which are entrained into the rising plumes and then trapped in the eddies. Within the eddies larvae are suspended in water with anomalous properties that may enhance survival.

Large-scale flow

Small-scale localized convection over the ridge crest can result in a large-scale circulation extending $O(1000\,\text{km})$ from the ridge. From the point of view of the large-scale mid-depth (2000–3000 m) circulation, venting at numerous locations along a ridge crest segment produces an average net upwelling localized over the ridge crest characterized by divergent isopycnals over the ridge crest. This can set up a mean circulation similar to the circulation from an individual vent plume, anticyclonic flow at the spreading level and cyclonic below, but now extending along the length of the ridge crest segment. Fluid entrained into the plumes and upwelled to the spreading level must be replaced. This requires a broad downwelling flow to close the mass balance. However, on these scales of 100–1000 km the variation of the Corriolis parameter due to the spherical shape of the earth, the β-effect, causes the two circulation cells to extend to the west of the ridge (regardless of hemisphere) to form what has been termed a β-plume. The ideal β-plume described here will be affected by the ridge crest topography and any background mid-depth flow. However, there is some observational evidence suggestive of this model of long-range dispersal of plume fluid. Observations near 15°S in the eastern Pacific (**Figure 8**) show a plume of anomalously high values of ^{3}He (a distinctive signature of hydrothermal origin water) centered in the water column just above the depth of the ridge crest. The plume extends over 2000 km west of the ridge. As predicted by the β-plume dynamics the westward extension of the plume is greatest closer to the equator. There are no similar observation in the Atlantic; this is perhaps explained by the deep axial topography.

Discussion

Localized high-temperature hydrothermal venting along ridge crest is capable of forcing circulations on scales many orders of magnitude larger than the vent field size. This is a consequence of the combination of the large buoyancy flux of hydrothermal vents and the dynamical effects of the Earth's rotation. Rotating flows are very sensitive to vertical motions such that small vertical flows are amplified into large horizontal circulations. The immense buoyancy flux of the high-temperature vents and megaplumes gives rise to rapid vertical ascent and just as importantly large entrainment of background fluid into the rising plumes. These combine to force a localized net upwelling many times larger than the mass flux of the individual vent. The stacked nature of the resulting horizontal flow, anticyclonic

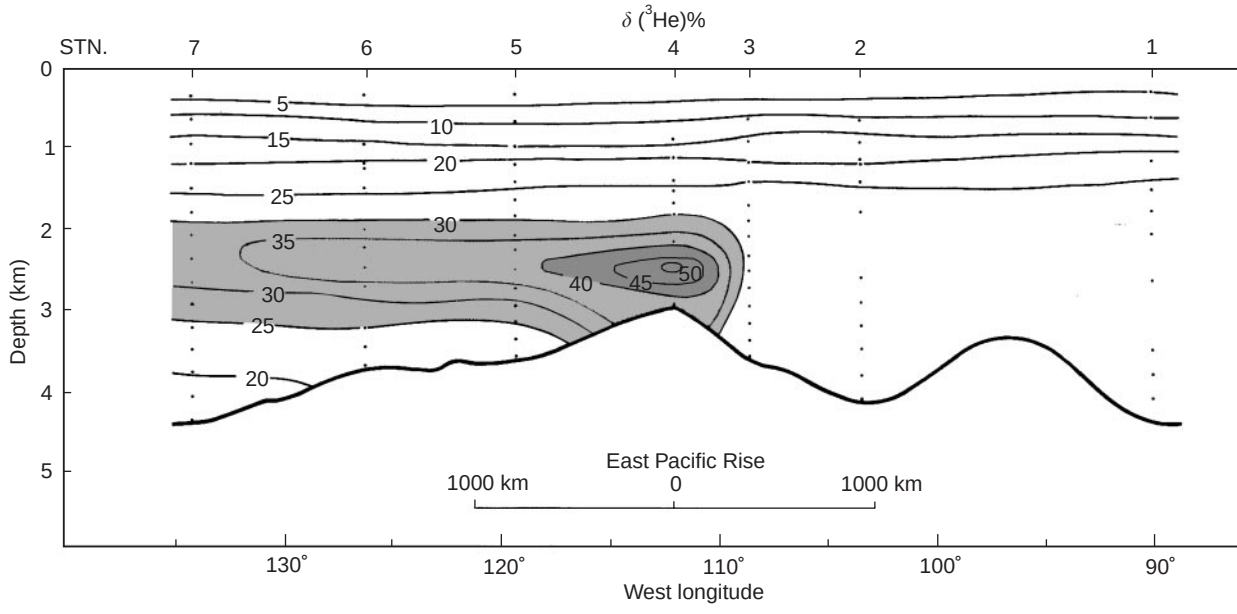

Figure 8 Transect along 15°S in the Pacific showing a plume of ^{3}He anomaly, $\delta(^3\text{He})$, extending over 2000 km west of the East Pacific Rise. (Reproduced with permission from Lupton, 1995.)

circulation at one level and cyclonic below, is typically unstable and produces eddies which have scales comparable to the local Rossby radius of deformation, $L_d = Z_M N/f$, based on the plume rise height. In reality the ultimate dispersion of high-temperature vent fluid probably occurs through a combination of simple advection and stirring by background flow and the formation of long-lived coherent vortices and β-plumes.

The reader might wonder whether these rotationally influenced convective processes are at work in the atmosphere where smokestacks and fires routinely cause localized plumes. There is one important difference between the atmosphere and the ocean in this regard. The scale at which rotation influences the flow and would produce eddies, the deformation radius L_d, is very much larger in the atmosphere than the ocean due to the greater static stability of the atmosphere (larger N). So these features are not likely to occur as a consequence of smokestacks and fires, which are simply too small to be affected by rotation. However, hurricanes are an example of the interaction of convection and rotation which produces intense vortices. Also, it would be possible for large volcanic eruptions which rise into the stratosphere to produce the atmospheric equivalent of oceanic megaplumes. Finally, oceanic deep convection produced by surface cooling and sinking induces some of the same circulation characteristics discussed here, but over typically much larger horizontal scales than isolated high-temperature vents.

List of Symbols

Z_M maximum plume rise height.
Z_s plume spreading level height.
F_0 source buoyancy flux.
N background buoyancy frequency.
g gravitational acceleration.
Q source volume flux.
ρ_0 density of the ambient fluid at vent level.
ρ_s source fluid density.
ρ_a ambient density.
z depth above the source.
θ latitude, potential temperature.
ϕ latitude.
H heat flux.
c_p specific heat at constant pressure.
T_s source temperature.
T_0 ambient temperature at vent level.
α coefficient of thermal expansion.
σ_2 measure of density.
B_0 initial buoyancy of a thermal.
V_0 initial volume of a thermal.
f Coriolis parameter.
Ω rotation rate of the Earth.
h vertical thickness of the anticyclonic plume eddy.
L radius of the anticyclonic plume eddy.
v azimuthal velocity within the plume eddy.
t_B timescale for plume break up.
L_d Rossby radius of deformation.

See also

Hydrothermal Vent Biota. Hydrothermal Vent Ecology. Hydrothermal Vent Fluids, Chemistry of. Meddies and Sub-surface Eddies. Mesoscale Eddies.

Further Reading

Baker ET and Massoth GJ (1987) Characteristics of hydrothermal plumes from two vent fields on the Juan de Fuca Ridge, northeast Pacific Ocean. *Earth and Planetary Science Letters* 85: 59–73.

Baker ET, Lavelle JW, Feely RA *et al.* (1989) Episodic venting of hydrothermal fluids from Juan de Fuca Ridge. *Journal of Geophysical Research* 94(B7): 9237–9250.

Helfrich KR and Battisti T (1991). Experiments on baroclinic vortex shedding from hydrothermal plumes. *Journal of Geophysical Research* 96: 12511–12518.

Humphries SE, Zierenberg RA, Mullineaux LS and Thomson RE (eds) (1995) *Seafloor Hydrothermal Systems, Physical, Chemical, Biological and Geological Interactions, Geophysical Monograph 91*. Washington, DC: American Geophysical Union.

Lupton JE (1995) Hydrothermal plumes: near and far field. In: Humphries SE, Zierenberg RA, Mullineaux LS and Thomson RE *Seafloor Hydrothermal Systems, Physical, Chemical, Biological and Geological Interactions*, pp. 317–346. *Geophysical Monograph 91*. Washington, DC: American Geophysical Union.

Lupton JE, Delaney JR, Johnson HP and Tivey MK (1985) Entrainment and vertical transport of deep-ocean water by buoyant hydrothermal plumes. *Nature* 316: 621–623.

Morton BR, Taylor GI and Turner JS (1956) Turbulent gravitational convection from maintained and instantaneous sources. *Proceedings of the Royal Society of London, Series A* 234: 1–13.

Parsons LM, Walker CL and Dixon DR (1995) *Hydrothermal Vents and Processes*. London: Geological Society.